Queuosine Salvage in *Bartonella henselae* Houston 1: A Unique Evolutionary Path

Samia Quaiyum[a%], Yifeng Yuan[a%], Guangxin Sun[b], R. M. Madhushi N. Ratnayake[c#] Geoffrey Hutinet[a@], Peter C. Dedon[b], Michael F. Minnick[d] and Valérie de Crécy-Lagard[a, e*]

[a] Department of Microbiology and Cell Science, University of Florida, Gainesville, FL 32611; [@]Current address: Department of Biology, Haverford College, 370 Lancaster Ave, Haverford, PA

[b] Department of Biological Engineering, Massachusetts Institute of Technology, Cambridge, MA 02139

[c] Department of Chemistry, University of Florida, Gainesville, FL 32611; [#]Current address: Department of Biochemistry, School of Medicine, Vanderbilt University, Nashville, TN 37232

[d] Division of Biological Sciences, University of Montana, Missoula, Montana, MT 59812

[e] Genetic Institute, University of Florida, FL 32611

[%]Contributed equally

*Corresponding author: vcrecy@ufl.edu

Short title: Queuosine salvage in Bartonella

Abstract

Queuosine (Q) stands out as the sole tRNA modification that can be synthesized via salvage pathways. Comparative genomic analyses identified specific bacteria that showed a discrepancy between the projected Q salvage route and the predicted substrate specificities of the two identified salvage proteins: 1) the distinctive enzyme tRNA guanine-34 transglycosylase (bacterial TGT, or bTGT), responsible for inserting precursor bases into target tRNAs; and 2) Queuosine Precursor Transporter (QPTR), a transporter protein that imports Q precursors. Organisms like the facultative intracellular pathogen *Bartonella henselae*, which possess only bTGT and QPTR but lack predicted enzymes for converting $preQ_1$ to Q, would be expected to salvage the queuine (q) base, mirroring the scenario for the obligate intracellular pathogen *Chlamydia trachomatis*. However, sequence analyses indicate that the substrate-specificity residues of their bTGTs resemble those of enzymes inserting $preQ_1$ rather than q. Intriguingly, mass spectrometry analyses of tRNA modification profiles in *B. henselae* reveal trace amounts of $preQ_1$, previously not observed in a natural context. Complementation analysis demonstrates that *B. henselae* bTGT and QPTR not only utilize $preQ_1$, akin to their *Escherichia coli* counterparts, but can also process q when provided at elevated concentrations. The experimental and phylogenomic analyses suggest that the Q pathway in *B. henselae* could represent an evolutionary transition among intracellular pathogens—from ancestors that synthesized Q *de novo* to a state prioritizing the salvage of q. Another possibility that will require further investigations is that the insertion of $preQ_1$ has fitness advantages when *B. henselae* is growing outside a mammalian host.

Keywords: Queuosine, *Bartonella henselae*, tRNA modification, intracellular parasite, TGT enzyme, YhhQ

Author summary

Transfer RNAs (tRNAs) are adaptors that deliver amino acids to ribosomes during translation of messenger RNAs (mRNAs) into proteins. tRNA molecules contain specially-modified nucleotides that affect many aspects of translation, including regulation of translational efficiency, as modified nucleotides primarily occur near the portion of tRNA (anticodon) that directly interacts with the coding sequence (codon) of the

mRNA while it is associated with a ribosome. Queuosine (Q) is a modified tRNA nucleotide located in the anticodon that can be synthesized or uniquely imported from the environment as Q or a precursor using a salvage mechanism. Free-living bacteria, e.g., *E. coli*, can synthesize Q or salvage precursors from the environment, but many obligate intracellular pathogens, e.g., *Chlamydia trachomatis*, cannot synthesize Q and must import a precursor from eukaryotic hosts. In this study, we determined that *Bartonella henselae*, a facultative intracellular bacterial pathogen of vascular cells, falls somewhere in the middle, as it is unable to synthesize Q but can salvage Q or certain precursors. The unusual nature of *Bartonella*'s system suggests different evolutionary scenarios. It could be a snapshot of the transition from Q synthesis to strict Q salvage or represent a unique adaptation to a complex multi-host lifestyle.

Introduction

tRNA modifications fine-tune translation by various mechanisms such as modulating the efficiency or accuracy of translation or affecting tRNA stability (1). Recent studies have revealed that modifications can play key roles in bacterial pathogenesis (2,3). Queuosine (Q) is a modification of the wobble base in tRNAs with GUN anticodons of many bacteria and eukaryotes that can affect both translational efficiency and accuracy depending on the organism (4,5). The *in vivo* significance of this modification has remained enigmatic for decades as it has been lost repeatedly during evolution (6), but recent studies have suggested that it may act as a regulatory component in the translation of proteins derived from genes enriched in TAT codons compared with TAC codons (7,8). In bacteria, Q modification was shown to have roles in oxidative stress, metal homeostasis, and virulence (9–12).

Q is synthesized from guanosine triphosphate (GTP) by bacteria in a complex eight-step pathway fully elucidated in *E. coli* (Fig. 1A). Four enzymes (GCHI, QueD, QueE, and QueC) convert GTP into 7-cyano-7-deazaguanine ($preQ_0$). QueF then reduces $preQ_0$ to 7-aminomethyl-7-deazaguanine ($preQ_1$) that is inserted into tRNAs by tRNA guanine-34 transglycosylase (bacterial TGT, or bTGT) (4). The inserted base $preQ_1$ is converted to Q by two additional steps involving QueA and QueG or QueH, depending on the

organism (4,13). It should be noted that Q is the only tRNA modification that can be salvaged or recycled (5). Eukaryotes only use the salvage route, and their TGT enzyme (eTGT), a heterodimeric QTRT1/QTRT2 complex, incorporates the queuine (q) base directly into the target tRNAs (5). The salvage routes in bacteria vary greatly. Some organisms lack the $preQ_0$ or $preQ_1$ pathway genes but encode all the downstream genes and import these precursor bases to finalize Q synthesis *in vivo* (14). This salvage route is also observed in organisms like *E. coli* that can synthesize Q *de novo*. Other bacteria lack all canonical synthesis genes except *tgt* and can salvage q like eukaryotes. Two q salvage routes have been identified in bacteria, to date (15), including the direct salvage route found in the intracellular pathogen *Chlamydia trachomatis*, or the indirect salvage route found in the gut microbe *Clostridioides difficile* (Fig. 1B and C, respectively). In the direct route, the substrate specificity of the *C. trachomatis* bTGT enzyme has shifted to insert q instead of $preQ_1$ like most bacterial homologs (15). In the indirect route, a recently discovered radical enzyme (QueL) can regenerate the $preQ_1$ intermediate from a q precursor that is imported directly or derived from the hydrolysis of the Q nucleoside by QueK (15). Only a few transporters involved in Q salvage pathways have been identified and experimentally characterized. The first was the YhhQ /COG1738 family, now renamed QPTR (Queuosine Precursor Transporter), involved in the transport of $preQ_0$ and $preQ_1$ in *E. coli* and q in *C. trachomatis* (14,15). Members of the Energy-Coupling Factors (ECFs) family had been predicted to be involved in $preQ_0$ and $preQ_1$ transports (15)) and two of the *C. difficile* specificity components (or ECF-QueT) were shown to transport a variety of Q precursors in a reconstituted system (15).

The proportion of Q-modified tRNAs can change with the developmental stage in several eukaryotic parasites that undergo complex cycles that switch between hosts such as *Trypanosoma cruzei* and *Entamoeba histolytica* (16,17). Very little is known about the role of Q in bacterial pathogens that also switch between mammalian and insect hosts such as the facultative intracellular pathogen *Bartonella henselae*. This bacterium uses fleas and possibly ticks as vectors during blood feeding. Feces of these insects can also infect cats when they are scratched into a break in the skin. Once inside the cat, the bacteria enter the bloodstream, primarily residing within endothelial cells, where they multiply (18). *B. henselae* exhibits

a high level of heterogeneity (19) and 16S rRNA sequence analyses led to the identification of two serotypes, Houston-1, and Marseille (20,21). Metabolic reconstruction of the Q synthesis pathway of *B. henselae* Houston 1 suggested it utilized a direct q salvage pathway like *C. trachomatis*. However, analysis of *B. henselae* bTGT and QTPR sequences did not match this prediction as these were more similar to the bTGT and QPTR enzymes that recognize $preQ_1$. To resolve this discrepancy, we set out to characterize experimentally the Q salvage enzymes in this facultative intracellular pathogen.

Results

Metabolic reconstruction and sequence analyses of queuosine salvage genes give contradictory results.

We previously showed that QPTR proteins have different substrate specificities, shifting from $preQ_0$ and $preQ_1$ in *E. coli* to q in *C. trachomatis* (14,15). To better understand the molecular determinants that drive this change in specificity, we constructed a Sequence Similarity Network (SSN) of the QPTR family (PF02592). We then colored the SSN based on the presence/absence of the Q synthesis genes in the corresponding genome as an indirect way to predict the substrate specificity of a given QPTR protein. As shown in Fig. 2, we were able to generate an SSN that separated the QPTR's predicted to salvage $preQ_0$ and $preQ_1$ (in yellow or red) from those predicted to salvage q (in blue). However, a few exceptions stood out even at a stringent alignment score of 70. The QPTRs found in organisms that encode only *tgt*, and hence predicted to salvage q, cluster with QPTR proteins predicted to salvage $preQ_0$/ $preQ_1$ because their genomes encode QueA and QueG or QueH (circled in Fig. 2). These include QPTR proteins from *Bartonella* species such as *B. henselae* Houston-1 (UniProt id A0A0H3M726_BARHE).

Following up on this discrepancy, we retrieved all Q synthesis proteins from the InterPro database with their IPR protein family ID (see Materials and Methods) and counted the numbers of each protein encoded in each genome at the level of different taxonomic ranks, including order, class, and family (Table S1). Then, we extracted the TGT sequences from all orders, classes, families, and genera that encode only

tgt as described in the methods section, aligned them, and compared the predicted substrate-binding residues (Table S2). As we previously reported (15), TGTs that salvage q typically contains GG[LS][AS]G in the substrate-binding pocket (Fig. 3). Interestingly, bTGTs in *Bartonella* and *Pelagibacter* contain a GGLAVG site like the *E. coli* enzyme (Fig. 3) and are phylogenetically distant from other bTGTs found in genomes that only encode *tgt* (Fig. 3). We then examined the substrate-binding pocket in a modeled structure of *B. henselae* bTGT (Bh bTGT, UniProt ID A0A0R4J8M4_BARHE) aligned with the structure of the human TGT catalytic subunit QTRT1 in complex with q (PDB ID: 6H45) (22). The aspartate residues and G216GLAVGE222 that are conserved in bTGT proteins of the *Hyphomicrobiales* order are in proximity to queuine (Fig. S1B and C). The predicted distance between V220 and the cis-diol groups of q is less than 1 Angstrom (Fig. S1C), suggesting that it may prevent the binding of q to *B. henselae* bTGT as in the *Zymomonas mobilis* TGT (23). We previously showed that *C. trachomatis* TGT salvages q and that its substrate-binding pocket can accommodate the larger substrate (15). Here, we propose that the bTGT protein and the QPTR transporter in *Bartonella* and *Pelagibacter* species salvage preQ$_1$, even though they lack, like *C. trachomatis*, the enzymes that make Q-tRNAs from preQ$_1$-tRNAs.

***B. henselae* bTGT and QPTR proteins preferentially salvage preQ$_1$ but also q and Q with low affinity.** The gene encoding the *B. henselae* Bh bTGT protein complemented the Q- phenotype of a *queDF tgt* deletion mutant of *E. coli* when expressed *in trans* and in the presence of exogenous preQ$_1$ even in low concentrations (down to 10 nM) (Fig. 4A). Similarly, Bh QPTR transported both preQ$_1$ and preQ$_0$ in an *E. coli* strain auxotrophic for preQ$_1$ and preQ$_0$ (Fig. 4B). These results confirmed our predictions based on the SSN that the *Bartonella* bTGT and QPTR proteins use preQ$_1$ as a substrate but do not match the metabolic reconstruction that predicted q salvage in *B. henselae*. Hence, we tested if this organism's bTGT and QPTR could have evolved a broader substrate specificity and use q as a substrate.

To test whether the QPTR and bTGT proteins of *B. henselae* can use q as a substrate, we used an *E. coli* strain that expresses the QPTR and/or the bTGT proteins of *C. trachomatis* that can only use q as a substrate (Fig. 1) (15). Salvage of q was observed when expressing both Bh *tgt* and *yhhQ* genes at

concentrations of q over 500 nM (Fig. 4C). When overexpressing the *E. coli yhhQ* gene, no such salvage of q was observed even at concentrations of 5 μM (Fig. 4C). However, if the *C. trachomatis* bTGT and QPTR proteins can salvage q when present at 100 nM, the Bh QPTR cannot (Fig. S2). These results showed that the Bh QPTR protein has acquired the capacity to transport q while retaining the $preQ_1/preQ_0$ specificity, but it is still not as efficient as the *C. trachomatis* QPTR transporter that is specific for q.

We then tested whether the Bh QPTR could transport the Q ribonucleoside by modeling with an *E. coli* strain expressing the *C. difficile* Q hydrolase (Cd *queK*) and q lyase (Cd *queL*) genes that allow Q to be salvaged by *E. coli* (Fig. 1) (15). Expressing only Bh QPTR allowed the salvage of Q only at extremely high concentrations (5 μM) (Fig. 4D). When the *C. difficile* Q transporter (Cd ECF_TAA', QueT) is expressed in this strain, Q can be salvaged when present at concentrations of 100 nM [(15) and (Fig. 4D].

Traces of $preQ_1$ can be detected in endogenous *B. henselae* tRNAs

The natural habitat of this intracellular pathogen (mammalian vasculature) should be richer in q than in $preQ_1$. We, therefore, analyzed by LC-MS/MS the tRNA modification profile of bulk tRNA extracted from *B. henselae* cells grown in sheep blood agar (HIBB) medium. The experiments were performed three times independently with conflicting results. The first two experiments were done to test the tRNA extraction protocols with an intracellular bacterium, using only one sample each time. Small amounts of $preQ_1$ and minute amounts of Q were detected the first time (but neither was present the second time (data not shown). Because cells were grown in the presence of sheep blood and serum, we had little control over the sources of Q or $preQ_1$; we, therefore, repeated the experiment a third time with 5 independent samples, adding 100 nM $preQ_1$ in three of the samples. As shown in Fig. 5, Fig. S3 and Table S3, small amounts of $preQ_1$ and Q were detected in all samples (around 1000 times less than in a typical *E. coli* sample). The exogenous addition of 100 nM $preQ_1$ did not make any difference. It is not possible to determine if the observed Q was derived from *B. henselae* tRNAs or from contaminating mammalian tRNAs, as eukaryotic-specific tRNA modifications such as $m^2{}_2G$, are detected in similar quantities (Table S3) and great variations in Q levels

were observed between samples. Nevertheless, the presence of preQ$_1$ cannot be explained by any contamination as mammalian host tRNAs never harbor this modification and other bacteria would not accumulate it, as preQ$_1$ had only been detected previously in *queA* mutants of *E. coli* (24). The low amounts detected suggest that the tRNAs are not fully modified, as the preQ$_1$ levels are 11%-40% of cmnm^{5}s^{2}U levels and 1.1%-2.8% of k^{2}C levels; two well-conserved bacterial modifications (25)(Fig. S4 and Table S3).

Early loss of Q pathway genes in the *Bartonellaceae* family within the *Hyphomicrobiales* order

B. henselae belongs to the Alphaproteobacteria class (25). This is a diverse Gram-negative taxon comprised of several phototrophic genera, several genera metabolizing C1-compounds (e.g., *Methylobacterium* spp.), symbionts of plants (e.g., *Rhizobium* spp.), endosymbionts of arthropods (*Wolbachia*) and intracellular pathogens (e.g., *Rickettsia*) (26). To better understand the evolution of the Q synthesis and salvage pathway in Alphaproteobacteria, we performed a phylogenetic distribution analysis of the corresponding genes in 2,127 different species with complete genome sequences from the class in the BV-BRC database as described in the methods section (Fig. S5). The tree suggests that there were three events involving the loss of preQ$_1$ synthesis genes: one occurred after the split between *Brucella* and *Bartonella* species (Fig. 6 and Fig. S5 node 1), one occurred after the split of *Pelagibacteraceae* (Fig. S5 and Fig S6 node 2), and one occurred after the split of *Anaplasmataceae* (Fig. S5 and Fig S6 node 3). This analysis revealed that most Alphaproteobacteria are prototrophic for Q, as 1,414 (64%) of the species analyzed encode the complete pathway. In addition, if the loss of the preQ$_1$ synthesis genes occurred sporadically in different branches, all the organisms analyzed, with the exception of *Bartonella*, harbored *tgt*, *queA*, and *queG* genes and hence were not predicted to salvage q. Focusing more specifically on the *Bartonella* genus using a similar analysis revealed a very different pattern (Fig. 6).

Among the 65 organisms in the *Bartonella* genus with available complete genomes, as of October 2023, only *Bartonella* sp. HY038, branching at the root of the genus, encoded the canonical *de novo* Q synthesis pathway. Most, like *B. henselae*, have lost all the genes but *tgt*. In addition, a more in-depth

analysis revealed fragmented *tgt* genes of several *B. quintana* strains (boxed in Fig. 6), suggesting these organisms have totally lost the capacity to make Q-modified tRNAs. This evolutionary scenario seems to be a recurring theme in intracellular bacteria like the *Rickettsiales*. While nearly all rickettsiae branching closer to the root retain the full pathway except for *queD* (collapsed in Fig. S6), other rickettsiae such as *Anaplasma*, *Ehrlichia*, and *Wolbachia*, have lost nearly the full pathway. However, cases of fragmented *tgt* genes are rare and only observed in a *Wolbachia* endosymbiont of *Cimex lectularius* (box in Fig. S5).

In summary, the phylogenic distribution analysis suggests that the direct ancestor of *Bartonella* species must have harbored the full Q pathway but that it was lost very early in the evolution of this clade. Most bacteria in this clade are predicted to transport and insert $preQ_1$ but without further conversion to Q. In addition, some species like *B. quintana* have lost the pathway completely (Fig. 6).

Discussion

Q is an ancient modification predicted to be present in the ancestors of bacteria (27). It is still present in most extant bacteria even if minimalist genetic codes can exist without this complex modification (28). Independent analyses of the genomes of bacteria in the human microbiome have shown that 90 to 95% of these organisms maintain the capacity to synthesize or salvage Q with around half encoding the full synthesis pathway (15,29). Many of the bacteria that have lost Q are organisms that have undergone a genome reduction process, where their genetic material has been streamlined over evolutionary time such as the parasitic *Mycoplasma* spp. or insect endosymbionts such as *Riesia pediculicola* (30,31).

Obligate intracellular human pathogens tend to have reduced genomes compared to their free-living ancestors as their metabolisms have adapted to a nutritionally rich niche (32). Regarding Q, the scenarios that one can envision in the transition to a strict intracellular lifestyle with access to the queuine precursor from the mammalian host are: 1) keeping the ancestral pathway; 2) losing the modification; or 3) switching to a queuine salvage route. We performed the metabolic reconstruction of Q metabolism in genera of strict intracellular human pathogens such as *Chlamydia* spp., members of the order Rickettsiales (*Anaplasma* spp., and *Rickettsia* spp.) and *Coxiella burnetii* (33,34). Indeed, examples of these three possible paths were

observed (Fig. 7): *Rickettsia* (Fig. 7A) and *Coxiella* (Table S5 line 267) have kept the full Q synthesis pathway; *Anaplasma* spp. (Fig. 7A), *Borrelia* (Fig. 7B), *Ehrlichia* spp. (Table S5 line 52), and *Chlamydia* (Table S5 line 212), kept only *tgt*. Most species in Mycobacteriales have totally lost the pathway genes except *tgt* (Fig. 7C).

The situation seen in *B. henselae* is not commonly observed in other intracellular bacteria and no other organisms in the Hyphomicrobiales order seem to follow the same pattern (Fig. 7D). Indeed, the presence of bTGT and QPTR homologs and the absence of QueA and QueG or QueH (Fig. 6) would suggest that these organisms salvage q like *C. trachomatis*, but the corresponding enzymes have retained their substrate specificity towards $preQ_1$ (Figs. 3 and 4). $PreQ_1$ is not a molecule found in mammalian cells (Brian Green, personal communication), and the fact that we were able to detect a small proportion of tRNAs carrying that modification when extracted from *B. henselae* cells grown in HIBB suggests this pathway is functional even if the source of $preQ_1$ remains a mystery and could be due to contamination with a $preQ_1$ synthesizing organism, an unknown source of $preQ_1$ in the culture medium, or from the activity of a yet-to-be-discovered q hydrolase (intracellular or possibly extracellular as q transport is not efficient as discussed below) (Fig. 1D). The low amount of $preQ_1$ modification (Table S3) suggests it does not play an important role in decoding accuracy under these conditions. The fact that *tgt* gene decay is observed in several organisms in this clade such as *B. quintana* reinforces this idea. A primary difference between *B. quintana* and *B. henselae* is their reservoir ecology. *B. quintana* uses only humans as a reservoir, whereas *B. henselae* is more promiscuous and frequently isolated from both cats and humans (35).

Another intriguing finding of this study is that the QPTR and bTGT enzymes of *B. henselae* can use q as a substrate when present at high concentrations (>500 nM), whereas the *E. coli* orthologs cannot. It is difficult to establish if such concentrations could be physiological, and we could not show with certainty that *B. henselae* tRNA extracted from HIBB-grown cells harbored Q. One can propose several evolutionary explanations for this broadening of substrate specificity of the *B. henselae* salvage proteins. In one, the enzyme and transporter specificities would become more relaxed in *B. henselae* as they are no longer under selective pressure to maintain efficient $preQ_1$ selection, and we are observing an intermediate stage along

the evolutionary loss of the whole pathway. An argument against that hypothesis is that if $preQ_1$ synthesis genes and *queA*, *queG* and *queH* genes seem to have been lost very early in the clade, *tgt* is often the last maintained and we did not find any examples where *tgt* was lost with the other genes maintained, suggesting a fitness advantage of maintaining the *tgt* gene. In addition, both *B. henselae* QPTR and bTGT encoding genes are expressed and the proteins detected *in vitro* [see Table S5 of (36)]. The other possibility is that we are observing a transition of a $preQ_1$ salvage to a q salvage that is working poorly in human cells but could be efficient in an environment with more q/Q. Could the insect vector provide such an environment? Answering these questions will require further studies, including additional quantitative data on q/$preQ_1$ levels in different environments and tRNA modification profiles along the pathogen's life cycle. In summary, the study sheds light on the diverse and adaptable nature of queuosine metabolism in various bacteria, particularly in intracellular pathogens. The unique characteristics of Q salvage observed in *B. henselae* raise intriguing questions about its role in different host/vector environments. Further investigations are warranted to unravel the complexities of Q salvage and its implications to *Bartonella*'s virulence.

Materials and methods

Comparative genomics and bioinformatics

The BLAST tools (37) resources at the National Center for Biotechnology Information (NCBI) and BV-BRC (38) were routinely used. Multiple sequence alignments were built using MUSCLE v5. 1 (39) and visualized and edited with Jalview2 (40). Protein sequences were retrieved from the NCBI using the following accession numbers: Ct YhhQ, NP_219643.1; Ct TGT, NP_219697.1; Cd ECF-A, YP_001086568.1; Cd ECF-A, YP_001086569.1; Cd ECF-T, YP_001086570.1; Cd Queuosine hydrolase, YP_001088185.1; Cd ECF-S, YP_001088186.1; Cd Queuine lyase, YP_001088187.1; Ec YhhQ, WP 001100469.1; Ec bTGT; Bh YhhQ, WP_011181356.; Bh bTGT, WP_011180873.1. Protein IDs used for this study are listed in Table S6. Complete genomes of Alphaproteobacteria with good quality were retrieved from BV-BRC (38).

For metabolic reconstruction analyses in each taxonomic rank, all protein members were retrieved from the InterPro database (41) using the following IPR family ID: FolE1, IPR001474; FolE2, IPR003801; QueD, IPR007115; QueE, IPR024924; QueC, IPR018317; QueF, IPR00029500; TGT, IPR004803; QueA, IPR003699; QueG, IPR004453; QueH, IPR003828. A universal single-copy small ribosomal protein uS2, (IPR001865) was used to estimate the number of organisms in each rank. The number of proteins per taxonomic rank was computed and the criteria used for filtering the groups ranks encoding just TGT were the following: 1) the number of TGT proteins was no less than 10 so we were not polluted with small taxonomic sample size; 2) the number of each of the QueDECFAGH proteins was no more than a fifth of the number of TGT proteins. To analyze the conserved residues in the substrate-binding pockets, the sequences of TGT proteins from select taxonomic groups were retrieved from UniProt and aligned using MUSCLE v5.1 (39). The conserved residues were visualized using weblogo3 (42).

The structure of TGT proteins (*Bartonella henselae* str. Houston-1 bTGT, A0A0R4J8M4; *Anaplasma phagocytophilum* bTGT, S6G6J1; *Nakamurella multipartita* bTGT, C8X7A7) were modeled using SWISS-MODEL (40) using Alpha Fold structure (*Bartonella fuyuanensis* bTGT (ID A0A840DZ06_9HYPH), *Anaplasma phagocytophilum* str ApMUC09 TGT (ID A0A0F3NAG3_ANAPH), and *Nakamurella multipartita* bTGT (ID C8X7A7_NAKMY) as templates respectively (43). The cartoon representation of protein structure was produced by PyMol (version 2.5) (44) and colored by domain (red, N-terminus; light blue, C-terminus).

Sequence Similarity Networks (SSNs)

The Enzyme Function Initiative (EFI) suite of web tools was used to generate the SSN (45). Visualization of SSNs was carried out using Cytoscape 3.10.1ape (46). 7,625 PF02592 family sequences were retrieved from UniProt using the family option with fraction of 3 and submitted to EFI. The initial SSN was generated with an alignment score cutoff set such that each connection (edge) represents a sequence identity of above approximately 40%. The obtained SSN was first colored according to the configurations for salvaging $preQ_1$, $preQ_0$, queuine, and Queuosine *de novo* synthesis. Then more stringent SSNs were created by

increasing the alignment score cutoff in small increments (usually by 5). This process was repeated until most clusters were homogeneous in their colors. The UniProt IDs were associated with the genome ID including GenBank/EMBL, RefSeq nucleotide, BV-BRC genome ID, Ensembl genome ID, using homemade scripts (scripts available upon request). The UniProt IDs of PF02592 family sequences in the SSN are listed in Table S7 as well as corresponding presence of Q pathway genes. The connection between UniProt IDs and genome information was performed by querying UniProt ID mapping file using homemade scripts (scripts available upon request).

Phylogenetic investigations and Q gene presence/absence distribution pattern analysis

For phylogenetic analysis of species, the 20 ribosomal protein data (L2, L3, L4, L5, L6, L9, L10, L14, L16, L18, L22, L24, S2, S3, S4, S5, S8, S10, S17, and S19) were retrieved from BV-BRC and aligned independently using MUSCLE v5.1 (39). Alignments were trimmed using BMGE v1.12 using default settings (47) and then concatenated. To build the phylogenetic tree of TGT proteins, the sequences of TGT proteins from each taxonomic rank were retrieved (ID are listed in Table S6) and subject to alignment with MUSCLE (39) and trimming with BMGE (47). The maximum likelihood tree was built by FastTree (48) using the LG-cat model with a hundred bootstraps. Trees were visualized using iTOL (49). To view the gene clustering near *tgt* in different bacterial genomes, GizmoGene (http://www.gizmogene.com) was used to extract gene regions and subjected to visualization using Gene Graphics (50). The genomic regions are listed in Table S4.

Strains, media, and growth conditions

Strains and plasmids used in this study are listed in Table S9. LB medium (tryptone 10 grams/liter, yeast extract 5 grams/liter, sodium chloride 5 grams/liter) was routinely used for *E. coli* growth at 37°C. The medium was solidified using 15 g/L of agar. As needed, kanamycin (50 g/mL), ampicillin (100 g/mL), and chloramphenicol (25 g/mL) were added. In the presence of exogenous Q precursors as previously described (51), cells were cultured in M9-defined medium containing 1% glycerol (Thermo Fisher Scientific,

Waltham, MA, USA) for the purpose of eliminating background Q-tRNA. After cells reached an optical density at 600 nm (OD_{600nm}) of 0.1-0.2, 0.2% arabinose was added to induce the expression of genes under the pBAD promoter. After cells reached an OD_{600nm} of 0.2, DMSO, $preQ_0$, $preQ_1$, q, or Q were added. The transport reaction was stopped at time points of 30 or 60 min after supplementing with DMSO or different Q precursors by placing samples on melting ice and then centrifuging, followed by tRNA extraction. Q was purchased from Epitoire (Singapore), q from Santa Cruz Biotechnology, $preQ_1$ and $preQ_0$ from Sigma-Aldrich.

B. henselae Houston I was obtained from the American Type Culture Collection (ATCC 49882) and cultivated as previously described (52) on HIBB agar plates [Bacto heart infusion agar (Becton, Dickinson, Sparks, MD) supplemented with 4% defibrinated sheep blood and 2% sheep serum (Quad Five, Ryegate, MT) by volume] for 4 days at 37ºC, 5% CO_2 and 100% relative humidity. When required, $preQ_1$ was added to a final concentration of 100 nM. Following harvest into ice-cold heart infusion broth, tRNA was collected from the bacterial cells.

Construction of *E. coli* strains and plasmids

B. henselae yhhQ gene (Bh *yhhQ*) was chemically synthesized (without optimization) in pTWIST-Kan vector. XbaI and HindIII restrictions sites were added at the 5′ and 3′ ends, respectively (Twist Bioscience HQ) (**Table S10**). Bh *yhhQ* DNA sequence was amplified using two primers pairs (F_Bh yhhQ_XbaI_PBAD33 and R_Bh yhhQ_HindIII_PBAD33) by PCR with the addition of restrictions sites XbaI and HindIII at their 5′ and 3′ ends, respectively. Bh *yhhQ* was cloned into the XbaI and HindIII sites of pBAD33. *B. henselae tgt* (Bh *tgt*) was amplified by PCR from *B. henselae* genomic DNA using the KpnI-RBS-TGTBh-F_PBAD24 and TGTBh-SbfI-R _PBAD24 primers and cloned into the KpnI and SbfI sites of pBAD24. The UniProt IDs for Bh *yhhQ* and Bh *tgt* are A0A0H3M726_BARHE and A0A0R4J8M4_BARHE, respectively. *E. coli* transformations were performed using the $CaCl_2$ chemical transformation procedure (53). Transformants were selected on LB agar supplemented with ampicillin or chloramphenicol (100 µg/mL). The clones were validated through sequencing and PCR analyses using

primers designed specifically for Bh *yhhQ* and Bh *tgt* genes. All primers used in this study are listed in Table S10.

tRNA extraction and migration

Cells were harvested by centrifugation at 16,000 x g for 2 minutes at 4°C. Immediately after pelleting, the cells were resuspended in 1 mL of Trizol (Thermo Fisher Scientific, Waltham, MA, USA). According to the manufacturer's instructions, small RNA was extracted with the PureLink^{Tm} miRNA Isolation kit (Thermo Fisher Scientific, Waltham, MA, USA). 50 µL of RNase-free water were used to elute the purified RNAs. Quantification of prepared tRNA was performed using a Nanodrop 1000 spectrophotometer. We loaded 150 ng of tRNAs per well on a denaturing 8 M urea, 8% polyacrylamide gel containing 0.5% 3-(Acrylamido) phenylboronic acid (Sigma-Aldrich) after resuspending in a 2X RNA Loading Dye (NEB). Migration was performed in a mixture of 1X TAE at 4°C. With a wet transfer apparatus in 1X TAE at 150 mA at 4°C for 90 minutes, tRNAs were transferred onto a Biodyne B precut nylon membrane (Thermo Scientific). The membrane was UV irradiated in a UV crosslinker (Fisher FB-UVXL-1000) at a preset UV energy dosage of 120 mJ/cm2. The North2South Chemiluminescent Hybridization and Detection Kit (Thermo) was used to detect $tRNA^{Asp}$. As the DIG Easy Hyb (Roche) drastically reduces the background noise, it was used as the initial membrane-blocking buffer instead of the North2South kit's membrane-blocking buffer. Hybridization was done at 60°C, using the specific biotinylated primer for tRNA Asp GUC (14) (5' biotin-CCCTGCGTGACAGGCAGG 3' for *E. coli* added to a final concentration of 50 ng/mL. The blot was visualized by the iBright™ Imaging Systems.

tRNA profiling by mass spectrometry

tRNA for each sample (1.8 µg) was hydrolyzed in a 30 µL digestion cocktail containing 2.49 U benzonase, 3 U CIAP (calf intestinal alkaline phosphatase), 0.07 U PDE I (phosphodiesterase I), 0.1 mM deferoxamine, 0.1 mM BHT (butylated hydroxytoluene), 3 ng coformycin, 25 nM 15N-dA (internal standard $[^{15}N]_5$-deoxyadenosine), 2.5 mM $MgCl_2$ and 5 mM Tris-HCL buffer pH 8.0. The digestion mixture was incubated

at 37 °C for 6 h. After digestion, all samples were analyzed by chromatography-coupled triple-quadrupole mass spectrometry (LC-MS/MS). For each sample, 600 ng of hydrolysate was injected for two technical replicates. Using synthetic standards, HPLC retention times of RNA modifications were confirmed on a Waters Acuity BEH C18 column (50 × 2.1 mm inner diameter, 1.7 µm particle size) coupled to an Agilent 1290 HPLC system and an Agilent 6495 triple-quad mass spectrometer. The Agilent sample vial insert was used. The HPLC system was operated at 25 °C and a flow rate of 0.3 mL/min in a gradient Table S11 with Buffer A (0.02% formic acid in double distilled water) and Buffer B (0.02% formic acid in 70% acetonitrile). The HPLC column was coupled to the mass spectrometer with an electrospray ionization source in positive mode with the following parameters: Dry gas temperature, 200 °C; gas flow, 11 L/min; nebulizer, 20 psi; sheath gas temperature, 300 °C; sheath gas flow, 12 L/min; capillary voltage, 3000 V; nozzle voltage, 0 V. Multiple reaction monitoring (MRM) mode was used for detection of product ions derived from the precursor ions for all the RNA modifications with instrument parameters including the collision energy (CE) optimized for maximal sensitivity for the modification. Based on synthetic standards (Biosynth) with optimized collision energies, the following transitions and retention times (except k^2C, which we do not have standard) were monitored: $cmnm^5s^2U$, m/z 348 → 141, 2.36 min; k^2C, m/z 372.1 → 240.1; $m^{2,2}G$, m/z 312 → 180, 9.70 min; $preQ_1$, m/z 312 → 163, 2.15 min; Q, m/z 410 → 163, 5.53 min. Signal intensities for each ribonucleoside were normalized by dividing by the sum of the UV signal intensities of the four canonical ribonucleosides recorded with an in-line UV spectrophotometer at 260 nm.

Conflicts of Interest

No conflicts of interest.

Funding Information

This work was funded by the National Institutes of Health (project numbers GM070641, ES026856, and ES024615) and the National Research Foundation of Singapore through the Singapore-MIT Alliance for Research and Technology Antimicrobial Resistance Interdisciplinary Research Group.

Acknowledgments

We are thankful to Dr Brian Greene for communicating unpublished results.

References

1. El Yacoubi B, Bailly M, de Crécy-Lagard V. Biosynthesis and function of posttranscriptional modifications of transfer RNAs. Annu Rev Genet. 2012 Dec 15;46(1):69–95.
2. Antoine L, Bahena-Ceron R, Bunwaree HD, Gobry M, Loegler V, Romby P, et al. RNA modifications in pathogenic bacteria: Impact on host adaptation and virulence. Vol. 12, Genes. MDPI AG; 2021. p. 1125.
3. Fleming BA, Blango MG, Rousek AA, Kincannon WM, Tran A, Lewis AJ, et al. A tRNA modifying enzyme as a tunable regulatory nexus for bacterial stress responses and virulence. Nucleic Acids Res. 2022 Jul 22;50(13):7570–90.
4. Hutinet G, Swarjo MA, de Crécy-Lagard V. Deazaguanine derivatives, examples of crosstalk between RNA and DNA modification pathways. Vol. 14, RNA Biology. Taylor and Francis Inc.; 2017. p. 1175–84.
5. Fergus C, Barnes D, Alqasem MA, Kelly VP. The queuine micronutrient: Charting a course from microbe to man. Vol. 7, Nutrients. MDPI AG; 2015. p. 2897–929.
6. Zallot R, Brochier-Armanet C, Gaston KW, Forouhar F, Limbach PA, Hunt JF, et al. Plant, animal, and fungal micronutrient queuosine is salvaged by members of the DUF2419 protein family. ACS Chem Biol. 2014 Aug 15;9(8):1812–25.
7. Chevance FFV, Le Guyon S, Hughes KT. The effects of codon context on in vivo translation speed. PLoS Genet. 2014;10(6):e1004392.
8. Whittle CA, Kulkarni A, Chung N, Extavour CG. Adaptation of codon and amino acid use for translational functions in highly expressed cricket genes. BMC Genomics. 2021 Dec 1;22(1):234.

9. Pollo-Oliveira L, Davis NK, Hossain I, Ho P, Yuan Y, Salguero García P, et al. The absence of the queuosine tRNA modification leads to pleiotropic phenotypes revealing perturbations of metal and oxidative stress homeostasis in *Escherichia coli* K12. Metallomics. 2022 Sep 24;14(9):mfac065.

10. Durand JM, Dagberg B, Uhlin BE, Björk GR. Transfer RNA modification, temperature and DNA superhelicity have a common target in the regulatory network of the virulence of *Shigella flexneri*: the expression of the *virF* gene. Mol Microbiol. 2000;35(4):924–35.

11. Díaz-Rullo J, González-Pastor JE. tRNA queuosine modification is involved in biofilm formation and virulence in bacteria. Nucleic Acids Res. 2023 Aug 28;51(18):9821–37.

12. Fruchard L, Babosan A, Carvalho A, Lang M, Li B, Duchateau M, et al. Queuosine modification of tRNA-Tyrosine elicits translational reprogramming and enhances growth of *Vibrio cholerae* with aminoglycosides. bioRxiv]. 2022 Jan 1;2022.09.26.509455.

13. Zallot R, Ross R, Chen WH, Bruner SD, Limbach PA, de Crécy-Lagard V. Identification of a novel epoxyqueuosine reductase family by comparative genomics. ACS Chem Biol. 2017 Feb 8;12(3):844–51.

14. Zallot R, Yuan Y, De Crécy-Lagard V. The *Escherichia coli* COG1738 member YhhQ is involved in 7-cyanodeazaguanine ($preQ_0$) transport. Biomolecules. 2017 Mar 1;7(1):12.

15. Yuan Y, Zallot R, Grove TL, Payan DJ, Martin-Verstraete I, Šepić S, et al. Discovery of novel bacterial queuine salvage enzymes and pathways in human pathogens. Proc Natl Acad Sci U S A. 2019 Sep 17;116(38):19126–35.

16. Guillén N. Pathogenicity and virulence of *Entamoeba histolytica*, the agent of amoebiasis. Vol. 14, Virulence. 2023. p. 2158656.

17. Dixit S, Kessler AC, Henderson J, Pan X, Zhao R, D'Almeida GS, et al. Dynamic queuosine changes in tRNA couple nutrient levels to codon choice in *Trypanosoma brucei*. Nucleic Acids Res. 2021 Dec 16;49(22):12986–99.

18. Jin X, Gou Y, Xin Y, Li J, Sun J, Li T, et al. Advancements in understanding the molecular and immune mechanisms of Bartonella pathogenicity. Front Microbiol. 2023 Jul 27;14:1196700.

19. Hansmann Y, DeMartino S, Piémont Y, Meyer N, Mariet P, Heller R, et al. Diagnosis of cat scratch disease with detection of *Bartonella henselae* by PCR: A study of patients with lymph node enlargement. J Clin Microbiol. 2005 Aug;43(8):3800–6.

20. La Scola B, Liang Z, Zeaiter Z, Houpikian P, Grimont PAD, Raoult D. Genotypic characteristics of two serotypes of *Bartonella henselae*. J Clin Microbiol. 2002;40(6):2002–8.

21. Zeaiter Z, Fournier PE, Raoult D. Genomic variation of *Bartonella henselae* strains detected in lymph nodes of patients with cat scratch disease. J Clin Microbiol. 2002;40(3):1023–30.

22. Johannsson S, Neumann P, Ficner R. Crystal structure of the human tRNA guanine transglycosylase catalytic subunit QTRT1. Biomolecules. 2018 Sep 1;8(3):81.

23. Stengl B, Reuter K, Klebe G. Mechanism and substrate specificity of tRNA-Guanine transglycosylases (TGTs): tRNA-modifying enzymes from the three different kingdoms of life share a common catalytic mechanism. Chem Bio Chem. 2005;6(11):1926–39.

24. Slany RK, Bosl M, Kersten H. Transfer and isomerization of the ribose moiety of AdoMet during the biosynthesis of queuosine tRNAs, a new unique reaction catalyzed by the QueA protein from *Escherichia coli*. Biochimie. 1994;76(5):389–93.

25. Boccaletto P, MacHnicka MA, Purta E, Pitkowski P, Baginski B, Wirecki TK, et al. MODOMICS: A database of RNA modification pathways. 2017 update. Nucleic Acids Res. 2018;46(D1):D303–7.

26. Ferla MP, Thrash JC, Giovannoni SJ, Patrick WM. New rRNA gene-based phylogenies of the Alphaproteobacteria provide perspective on major groups, mitochondrial ancestry and phylogenetic instability. PLoS One. 2013 Dec 11;8(12):e83383.

27. Cermakian N, Cedergren R. Modified nucleosides always were: an evolutionary model. In: Grosjean H, Benne R, editors. Modification and Editing of RNA. Washington, D. C.: ASM Press; 1998. p. 535–41.

28. Garzón MJ, Reyes-Prieto M, Gil R. The minimal translation machinery: what we can learn from naturally and experimentally reduced genomes. Front Microbiol. 2022;13:858983.

29. Yan F, Xiang S, Shi L, Zhu X. Synthesis of queuine by colonic gut microbiome via cross-feeding. Food Frontiers1. 2023 Sep 15;1–14.

30. Grosjean H, Breton M, Sirand-Pugnet P, Tardy F, Thiaucourt F, Citti C, et al. Predicting the minimal translation apparatus: lessons from the reductive evolution of Mollicutes. PLoS Genet. 2014;10(5).

31. de Crécy-Lagard V, Marck C, Grosjean H. Decoding in Candidatus *Riesia pediculicola*, close to a minimal tRNA modification set? Trends Cell Mol Biol. 2012; 7:11–34.

32. Murray GGR, Charlesworth J, Miller EL, Casey MJ, Lloyd CT, Gottschalk M, et al. Genome reduction Is associated with bacterial pathogenicity across different scales of temporal and ecological divergence. Mol Biol Evol. 2021;38(4):1570–9.

33. McClure EE, Chávez ASO, Shaw DK, Carlyon JA, Ganta RR, Noh SM, et al. Engineering of obligate intracellular bacteria: Progress, challenges and paradigms. Vol. 15, Nature Reviews Microbiology. 2017. p. 544–58.

34. Loterio RK, Zamboni DS, Newton HJ. Keeping the host alive - Lessons from obligate intracellular bacterial pathogens. Vol. 79, Pathogens and Disease. 2021. p. ftab052.

35. Alsmark CM, Frank AC, Karlberg EO, Legault BA, Ardell DH, Canbäck B, et al. The louse-borne human pathogen *Bartonella quintana* is a genomic derivative of the zoonotic agent *Bartonella henselae*. Proc Natl Acad Sci U S A. 2004;101(26):9716–21.

36. Omasits U, Quebatte M, Stekhoven DJ, Fortes C, Roschitzki B, Robinson MD, et al. Directed shotgun proteomics guided by saturated RNA-seq identifies a complete expressed prokaryotic proteome. Genome Res. 2013 Nov;23(11):1916–27.

37. Altschul SF, Madden TL, Schaffer AA, Zhang J, Zhang Z, Miller W, et al. Gapped BLAST and PSI-BLAST: a new generation of protein database search programs. Nucleic Acids Res. 1997;25(17):3389–402.

38. Olson RD, Assaf R, Brettin T, Conrad N, Cucinell C, Davis JJ, et al. Introducing the Bacterial and Viral Bioinformatics Resource Center (BV-BRC): a resource combining PATRIC, IRD and ViPR. Nucleic Acids Res. 2023 Jan 6;51(D1):D678–89.

39. Edgar RC. Muscle5: High-accuracy alignment ensembles enable unbiased assessments of sequence homology and phylogeny. Nat Commun. 2022 Nov 15;13(1):6968.

40. Waterhouse AM, Procter JB, Martin DMA, Clamp M, Barton GJ. Jalview Version 2-A multiple sequence alignment editor and analysis workbench. Bioinformatics. 2009;25(9):1189–91.

41. Paysan-Lafosse T, Blum M, Chuguransky S, Grego T, Pinto BL, Salazar GA, et al. InterPro in 2022. Nucleic Acids Res. 2023 Jan 6;51(D1):D418–27.

42. Crooks GE, Hon G, Chandonia JM, Brenner SE. WebLogo: A Sequence Logo Generator. Genome Res 2004;14(6):1188–90.

43. Varadi M, Anyango S, Deshpande M, Nair S, Natassia C, Yordanova G, et al. AlphaFold Protein Structure Database: Massively expanding the structural coverage of protein-sequence space with high-accuracy models. Nucleic Acids Res. 2022 Jan 7;50(D1):D439–44.

44. Zhu K, Day T, Warshaviak D, Murrett C, Friesner R, Pearlman D. Antibody structure determination using a combination of homology modeling, energy-based refinement, and loop prediction. Proteins: Structure, Function and Bioinformatics. 2014;82(8):1646–55.

45. Gerlt JA, Bouvier JT, Davidson DB, Imker HJ, Sadkhin B, Slater DR, et al. Enzyme function initiative-enzyme similarity tool (EFI-EST): A web tool for generating protein sequence similarity networks. Vol. 1854, Biochimica et Biophysica Acta - Proteins and Proteomics. Elsevier B.V.; 2015. p. 1019–37.

46. Shannon P, Markiel A, Ozier O, Baliga NS, Wang JT, Ramage D, et al. Cytoscape: A software Environment for integrated models of biomolecular interaction networks. Genome Res. 2003 Nov;13(11):2498–504.

47. Criscuolo A, Gribaldo S. BMGE (Block Mapping and Gathering with Entropy): a new software for selection of phylogenetic informative regions from multiple sequence alignments. BMC Evol Biol. 2010;10:210.

48. Price MN, Dehal PS, Arkin AP. FastTree 2 – approximately maximum-likelihood trees for large alignments. PLoS One. 2010 Mar 10;5(3):e9490.

49. Letunic I, Bork P. Interactive tree of life (iTOL) v5: An online tool for phylogenetic tree display and annotation. Nucleic Acids Res. 2021;49(W1):W293–6.

50. Harrison KJ, de Crécy-Lagard V, Zallot R. Gene Graphics: A genomic neighborhood data visualization web application. Bioinformatics. 2018;34(8):1406–8.

51. Kelley LA, Mezulis S, Yates CM, Wass MN, Sternberg MJE. The Phyre2 web portal for protein modeling, prediction and analysis. Nat Protoc. 2015 Jun 30;10(6):845–58.

52. Battisti JM, Minnick MF. Laboratory maintenance of *Bartonella quintana*. Curr Protoc Microbiol. 2008 Aug;10(1):3C.1.1-3C.1.13.

53. Green R, Rogers EJ. Transformation of chemically competent *E. coli*. In: Methods in Enzymology. Academic Press Inc.; 2013. p. 329–36.

Figure legends

Fig 1. Known or predicted Q synthesis pathways.

(A) $preQ_0$/$preQ_1$ synthesis and salvage pathways in *E. coli*; (B) q salvage pathway in *C. trachomatis*; (C) $preQ_1$, q and Q salvage pathways in *C. difficile*. The ECF transporters include 4 subunits: S, the substrate-specific transmembrane component (QueT); T, the energy-coupling module; A and A', a pair of ABC ATPase. (D) Possible q and Q salvage pathways in *B. henselae* Houston 1.

Figure 2. Protein sequence similarity network (SSN) of 7,625 QPTR (PF02592 family) proteins.

Each node in the network represents a QPTR protein. An edge (represented as a line) is drawn between two nodes with a BLAST *E*-value cutoff of better than 10^{-70} (alignment score of 70). The nodes are colored based on the presence/absence of the other Q synthesis genes in the corresponding genome. Cases with inconclusive Q pathway gene distribution are colored in light gray. QPTR proteins without genome information are colored in dark gray. QPTR homologs from *E. coli* and *C. trachomatis* are indicated by yellow and blue arrows, respectively. The solitary TGTs from genomes harboring only *tgt* that cluster with TGTs in complete Q pathways are circled in blue.

Figure 3. Comparison of the phylogenetic tree of taxonomic ranks of bacteria that harbor *tgt* only and the maximum likelihood tree of their TGT proteins.

The maximum likelihood tree of marker proteins of taxonomic ranks of bacteria that harbor *tgt* only without other Q proteins (left). The maximum likelihood tree of TGT proteins from organisms of each corresponding rank (right). Human and *Pyrococcus horikoshii* tRNA-guanine (15) transglycosylases were used as the outgroup for each tree, respectively. TGT of *E. coli* was used for comparison. Bootstraps above 0.5 are shown under the branch. A multiple sequence alignment of consensus residues in the TGT proteins in the moiety of 7-substitue of deazapurine is shown (middle). The residues are highlighted by the percent identity. The dashed lines connect each organism and their TGT sequence. The branch of TGTs from *Bartonella, Pelagibacter, E. coli*, and humans is highlighted in red.

Figure 4. Bh TGT and Bh YhhQ salvage preQ$_1$ in *E. coli*.

Detection of Q-tRNAAsp GUC by the APB assay. Q-modified tRNAs that migrate slower are indicated by an arrow. tRNAs were extracted from WT and mutant strains expressing different Q salvage genes. The strains used are denoted in the first line. The genes and corresponding vectors are indicated in the second line. Plasmid and strain information are given in Table S9. Cells were grown in minimal media in the presence of exogenous preQ$_0$, preQ$_1$, q or Q as noted. DMSO was used as control when no deazapurine was supplemented.

Figure 5. Quantification of preQ1 and Q in *B. henselae*.

LC-MS/MS analysis of ribonucleosides containing preQ1 and Q was performed on 600 ng of hydrolyzed small RNA, with signal intensities normalized to the sum of UV absorbances of the canonical ribonucleosides, using an inline UV detector, to correct for differences in amounts of injected RNA. Data represent mean ± SD for three biological replicates of *B. henselae* BH-WT+preQ1 (BH-WT+preQ1) and mean ± deviation about the mean for two biological replicates of *B. henselae* BH-WT (BH-WT); technical duplicates were performed for each biological replicate. All modifications were validated with standards.

Figure 6. Phylogenetic analysis of Queuosine biosynthesis genes in *Bartonellaceae*. The clade of *Bartonella spp.* (*Bartonellaceae*; Alphaproteobacteria; left). The branches of *Pseudochrobactrum*, *Brucella*, and *Ochrobactrum* were collapsed. The highlighted node 1 corresponds to the node in the tree in Figure S5. The presence of Q biosynthesis proteins is indicated by the circles with TGTs highlighted in red. The comparative view of the corresponding truncated and full-length *tgt* gene variants in different *Bartonella* species in the tree (right). Red, *tgt*; yellow, *queA*; blue, genes encoding a transporter-like protein; black, hypothetical genes; gray, other genes. The fragmented *tgt* genes in *B. quintana* strains are boxed. Gene IDs are provided in supplementary Table S4.

Figure 7. The prevalence of Q pathway proteins in selected taxonomic ranks in Uniprot database.

(A) A cladogram of the order Hyphomicrobiales. (B) A cladogram of the order Mycobacteriales. (C) A cladogram of the class Spirochaetia. (D) A cladogram of the order Rickettsiales. Each pie chart represents the percentage of organisms in each taxonomic rank that contains the corresponding Q pathway protein. The size of each triangle correlates with the number of genomes in each taxonomic unit. The sequences of TGTs' substrate binding sites from ranks that encoded only *tgt* were analyzed and presented in Table. S2. Only taxonomic ranks that contain more than 15 TGTs are shown.

Figure 1

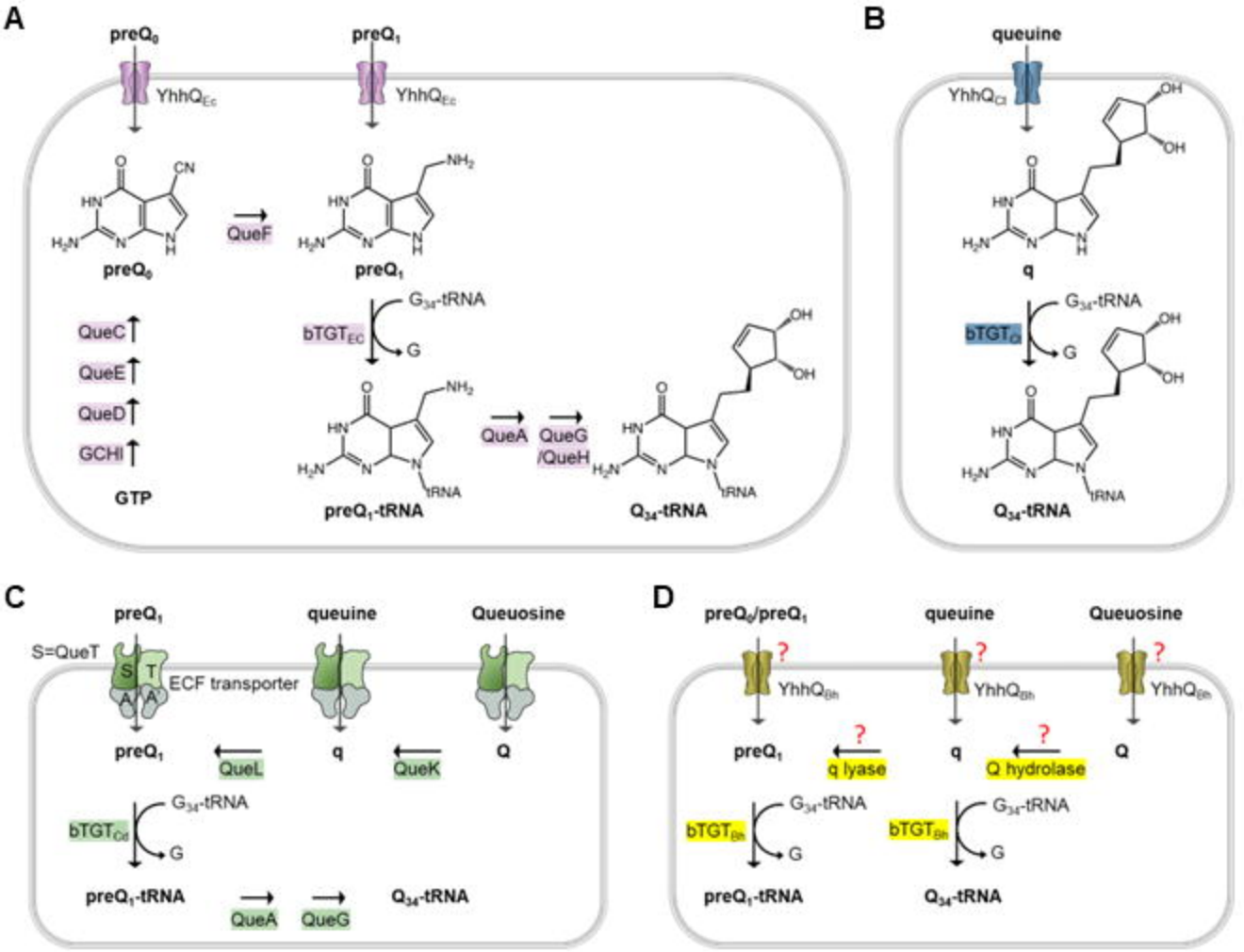
A
preQ0
preQ1
YhhQEc
YhhQEc
QueF
preQ0
preQ1
QueC
QueE
QueD
GCHI
GTP
G34-tRNA
bTGTEC
G
preQ1-tRNA
QueA
QueG
/QueH
Q34-tRNA
B
queuine
YhhQCl
q
G34-tRNA
bTGTCl
G
Q34-tRNA
C
preQ1
queuine
Queuosine
S=QueT
ECF transporter
preQ1
q
Q
QueL
QueK
G34-tRNA
bTGTCd
G
preQ1-tRNA
QueA
QueG
Q34-tRNA
D
preQ0/preQ1
queuine
Queuosine
YhhQBh
YhhQBh
YhhQBh
preQ1
q
Q
q lyase
Q hydrolase
G34-tRNA
bTGTBh
G
G34-tRNA
bTGTBh
G
preQ1-tRNA
Q34-tRNA

Figure 2

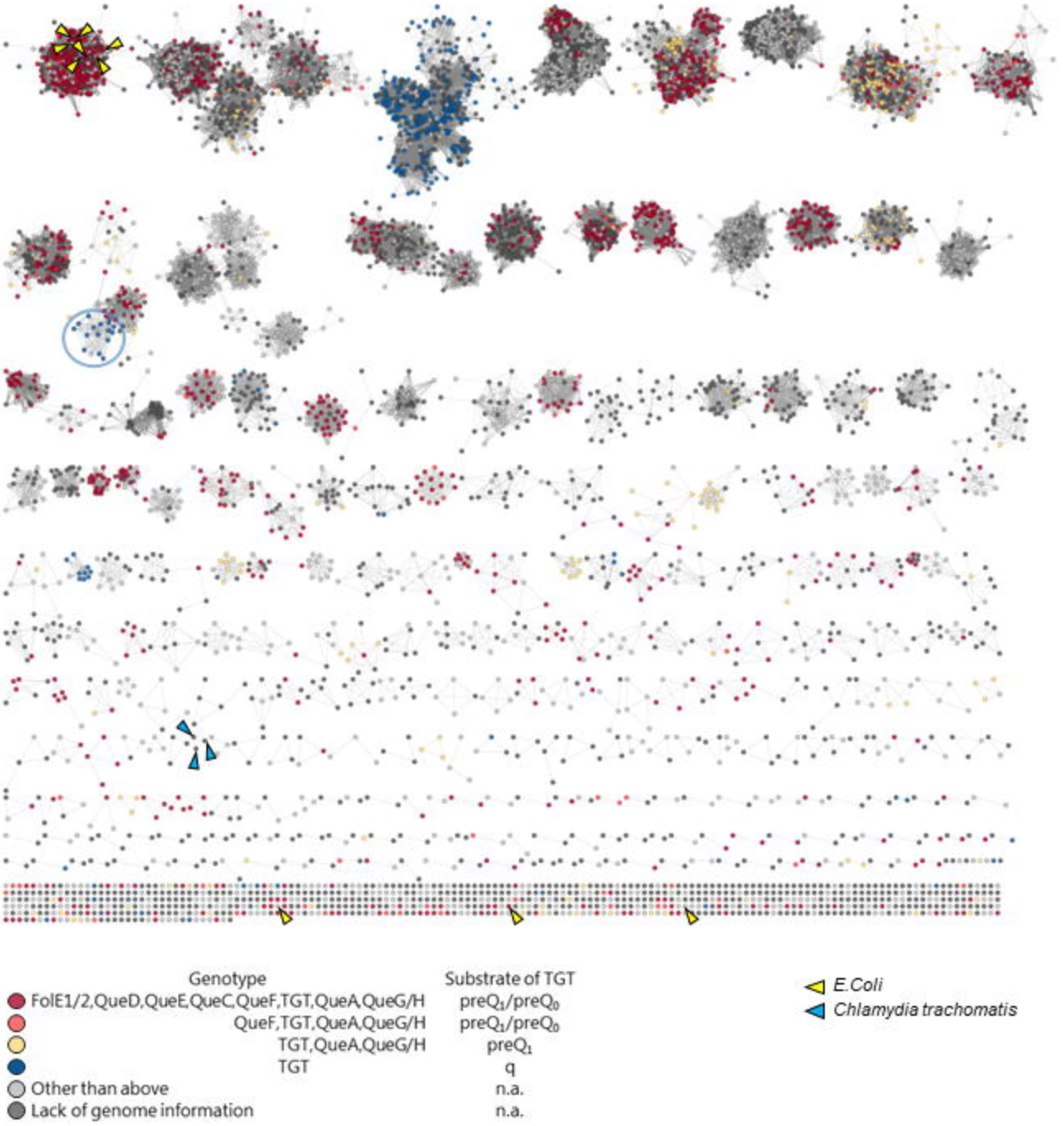
Genotype
Substrate of TGT
FolE1/2,QueD,QueE,QueC,QueF,TGT,QueA,QueG/H
preQ1/preQ0
QueF,TGT,QueA,QueG/H
preQ1/preQ0
TGT,QueA,QueG/H
preQ1
TGT
q
Other than above
n.a.
Lack of genome information
n.a.
E.Coli
Chlamydia trachomatis

Figure 3

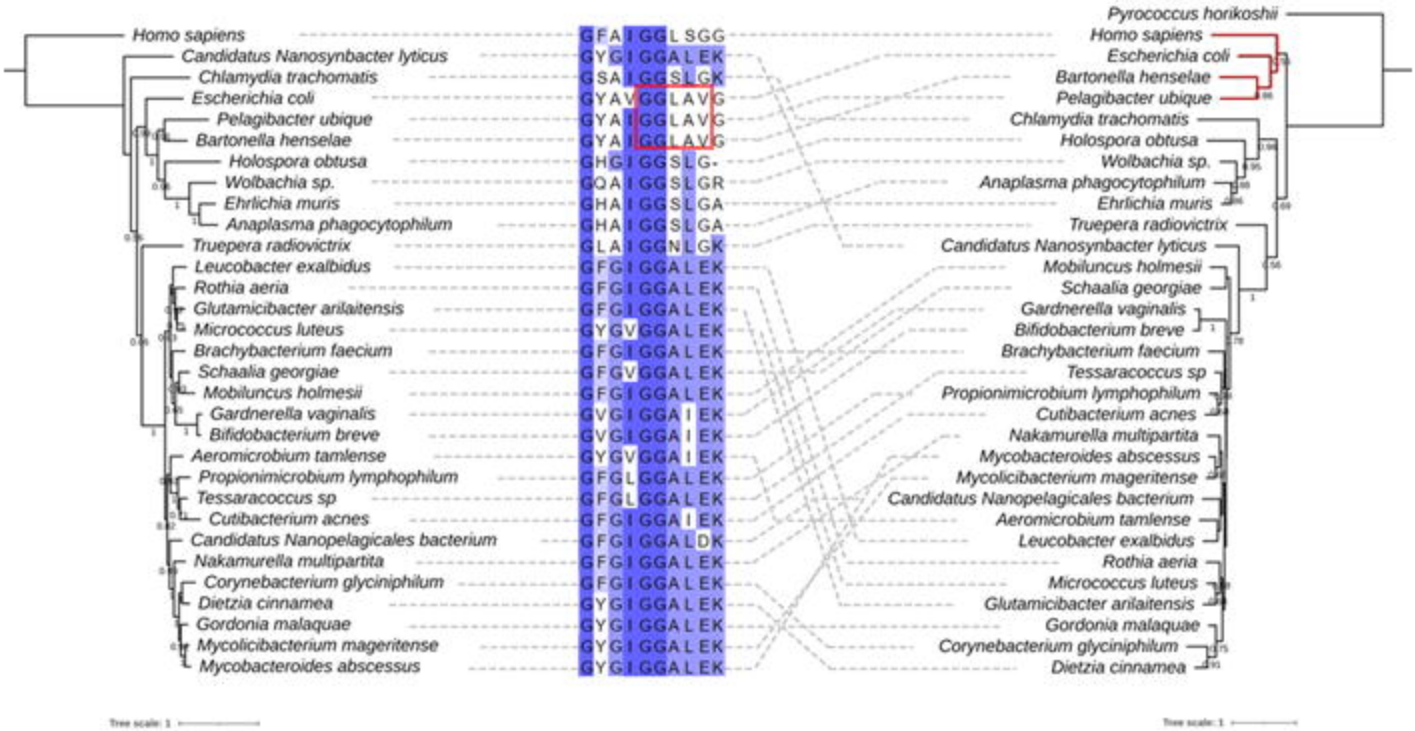
Homo sapiens GFAIGGLSGG
Candidatus Nanosynbacter lyticus GYGIGGALEK
Chlamydia trachomatis GSAIGGSLGK
Escherichia coli GYAVGGLAVG
Pelagibacter ubique GYAIGGLAVG
Bartonella henselae GYAIGGLAVG
Holospora obtusa GHGIGGSLG-
Wolbachia sp. GQAIGGSLGR
Ehrlichia muris GHAIGGSLGA
Anaplasma phagocytophilum GHAIGGSLGA
Truepera radiovictrix GLAIGGNLGK
Leucobacter exalbidus GFGIGGALEK
Rothia aeria GFGIGGALEK
Glutamicibacter arilaitensis GFGIGGALEK
Micrococcus luteus GYGVGGALEK
Brachybacterium faecium GFGIGGALEK
Schaalia georgiae GFGVGGALEK
Mobiluncus holmesii GFGIGGALEK
Gardnerella vaginalis GVGIGGAIEK
Bifidobacterium breve GVGIGGAIEK
Aeromicrobium tamlense GYGVGGAIEK
Propionimicrobium lymphophilum GFGLGGALEK
Tessaracoccus sp GFGLGGALEK
Cutibacterium acnes GFGIGGAIEK
Candidatus Nanopelagicales bacterium GFGIGGALDK
Nakamurella multipartita GFGIGGALEK
Corynebacterium glyciniphilum GFGIGGALEK
Dietzia cinnamea GYGIGGALEK
Gordonia malaquae GYGIGGALEK
Mycolicibacterium mageritense GYGIGGALEK
Mycobacteroides abscessus GYGIGGALEK
Pyrococcus horikoshii
Homo sapiens
Escherichia coli
Bartonella henselae
Pelagibacter ubique
Chlamydia trachomatis
Holospora obtusa
Wolbachia sp.
Anaplasma phagocytophilum
Ehrlichia muris
Truepera radiovictrix
Candidatus Nanosynbacter lyticus
Mobiluncus holmesii
Schaalia georgiae
Gardnerella vaginalis
Bifidobacterium breve
Brachybacterium faecium
Tessaracoccus sp
Propionimicrobium lymphophilum
Cutibacterium acnes
Nakamurella multipartita
Mycobacteroides abscessus
Mycolicibacterium mageritense
Candidatus Nanopelagicales bacterium
Aeromicrobium tamlense
Leucobacter exalbidus
Rothia aeria
Micrococcus luteus
Glutamicibacter arilaitensis
Gordonia malaquae
Corynebacterium glyciniphilum
Dietzia cinnamea
Tree scale: 1
Tree scale: 1

Figure 4

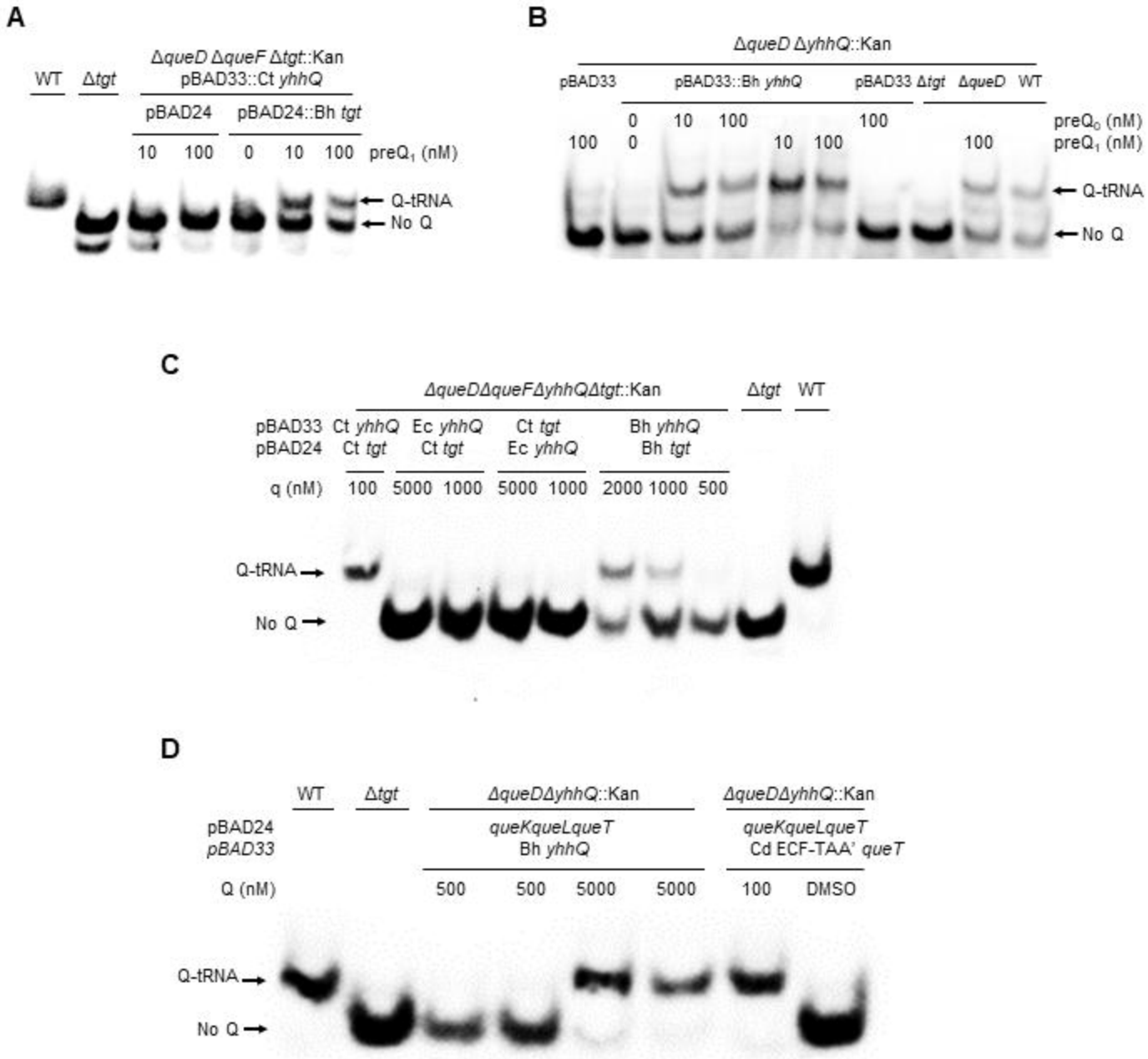
A
WT
Δtgt
ΔqueD ΔqueF Δtgt::Kan
pBAD33::Ct yhhQ
pBAD24
pBAD24::Bh tgt
10 100 0 10 100 preQ1 (nM)
Q-tRNA
No Q
B
ΔqueD ΔyhhQ::Kan
pBAD33
pBAD33::Bh yhhQ
pBAD33 Δtgt
ΔqueD
WT
0 10 100 100 preQ0 (nM)
100 0 10 100 100 preQ1 (nM)
Q-tRNA
No Q
C
ΔqueDΔqueFΔyhhQΔtgt::Kan
Δtgt
WT
pBAD33 Ct yhhQ Ec yhhQ Ct tgt Bh yhhQ
pBAD24 Ct tgt Ct tgt Ec yhhQ Bh tgt
q (nM) 100 5000 1000 5000 1000 2000 1000 500
Q-tRNA
No Q
D
WT
Δtgt
ΔqueDΔyhhQ::Kan
ΔqueDΔyhhQ::Kan
pBAD24 queKqueLqueT queKqueLqueT
pBAD33 Bh yhhQ Cd ECF-TAA' queT
Q (nM) 500 500 5000 5000 100 DMSO
Q-tRNA
No Q

Figure 5

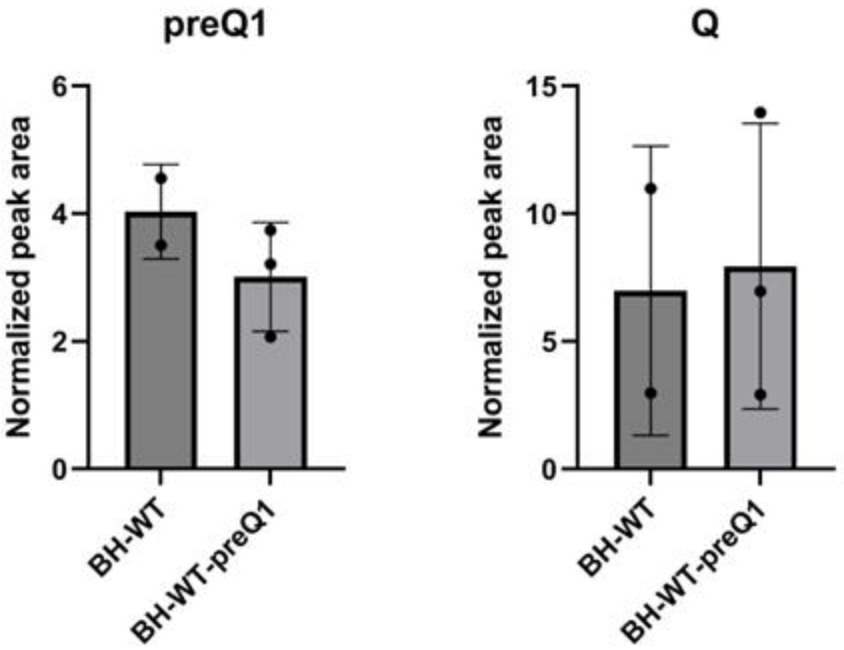
preQ1
Normalized peak area
6
4
2
0
BH-WT
BH-WT-preQ1
Q
Normalized peak area
15
10
5
0
BH-WT
BH-WT-preQ1

Figure 6

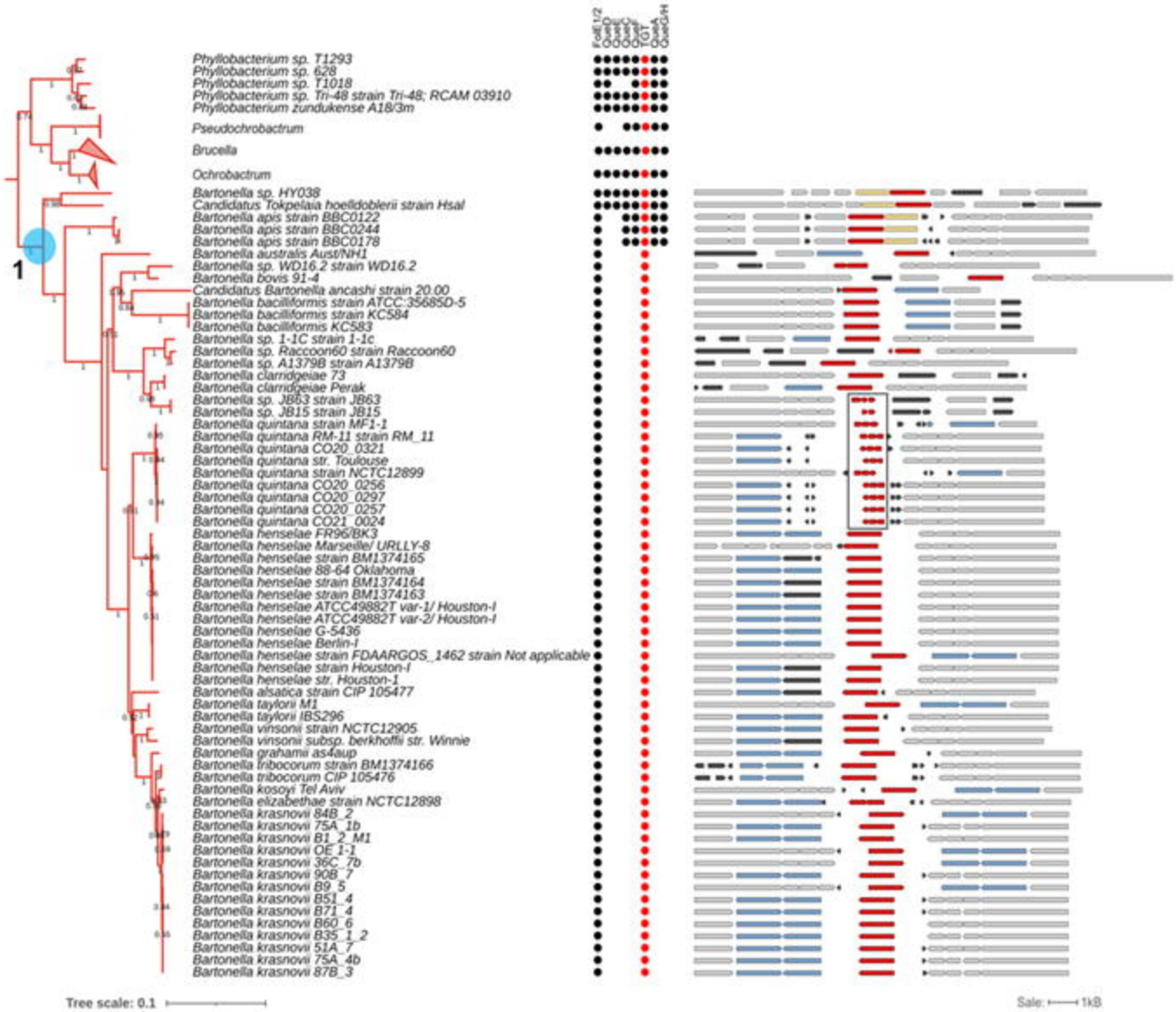

FolE1/2
QueD
QueE
QueC
QueF
TGT
QueA
QueG/H
Phyllobacterium sp. T1293
Phyllobacterium sp. 628
Phyllobacterium sp. T1018
Phyllobacterium sp. Tri-48 strain Tri-48; RCAM 03910
Phyllobacterium zundukense A18/3m
Pseudochrobactrum
Brucella
Ochrobactrum
Bartonella sp. HY038
Candidatus Tokpelaia hoelldoblerii strain Hsal
Bartonella apis strain BBC0122
Bartonella apis strain BBC0244
Bartonella apis strain BBC0178
Bartonella australis Aust/NH1
Bartonella sp. WD16.2 strain WD16.2
Bartonella bovis 91-4
Candidatus Bartonella ancashi strain 20.00
Bartonella bacilliformis strain ATCC:35685D-5
Bartonella bacilliformis strain KC584
Bartonella bacilliformis KC583
Bartonella sp. 1-1C strain 1-1c
Bartonella sp. Raccoon60 strain Raccoon60
Bartonella sp. A1379B strain A1379B
Bartonella clarridgeiae 73
Bartonella clarridgeiae Perak
Bartonella sp. JB63 strain JB63
Bartonella sp. JB15 strain JB15
Bartonella quintana strain MF1-1
Bartonella quintana RM-11 strain RM_11
Bartonella quintana CO20_0321
Bartonella quintana str. Toulouse
Bartonella quintana strain NCTC12899
Bartonella quintana CO20_0256
Bartonella quintana CO20_0297
Bartonella quintana CO20_0257
Bartonella quintana CO21_0024
Bartonella henselae FR96/BK3
Bartonella henselae Marseille/ URLLY-8
Bartonella henselae strain BM1374165
Bartonella henselae 88-64 Oklahoma
Bartonella henselae strain BM1374164
Bartonella henselae strain BM1374163
Bartonella henselae ATCC49882T var-1/ Houston-I
Bartonella henselae ATCC49882T var-2/ Houston-I
Bartonella henselae G-5436
Bartonella henselae Berlin-I
Bartonella henselae strain FDAARGOS_1462 strain Not applicable
Bartonella henselae strain Houston-I
Bartonella henselae str. Houston-1
Bartonella alsatica strain CIP 105477
Bartonella taylorii M1
Bartonella taylorii IBS296
Bartonella vinsonii strain NCTC12905
Bartonella vinsonii subsp. berkhoffii str. Winnie
Bartonella grahamii as4aup
Bartonella tribocorum strain BM1374166
Bartonella tribocorum CIP 105476
Bartonella kosoyi Tel Aviv
Bartonella elizabethae strain NCTC12898
Bartonella krasnovii 84B_2
Bartonella krasnovii 75A_1b
Bartonella krasnovii B1_2_M1
Bartonella krasnovii OE_1-1
Bartonella krasnovii 36C_7b
Bartonella krasnovii 90B_7
Bartonella krasnovii B9_5
Bartonella krasnovii B51_4
Bartonella krasnovii B71_4
Bartonella krasnovii B60_6
Bartonella krasnovii B35_1_2
Bartonella krasnovii 51A_7
Bartonella krasnovii 75A_4b
Bartonella krasnovii 87B_3
1
Tree scale: 0.1
Sale: 1kB

Figure 7

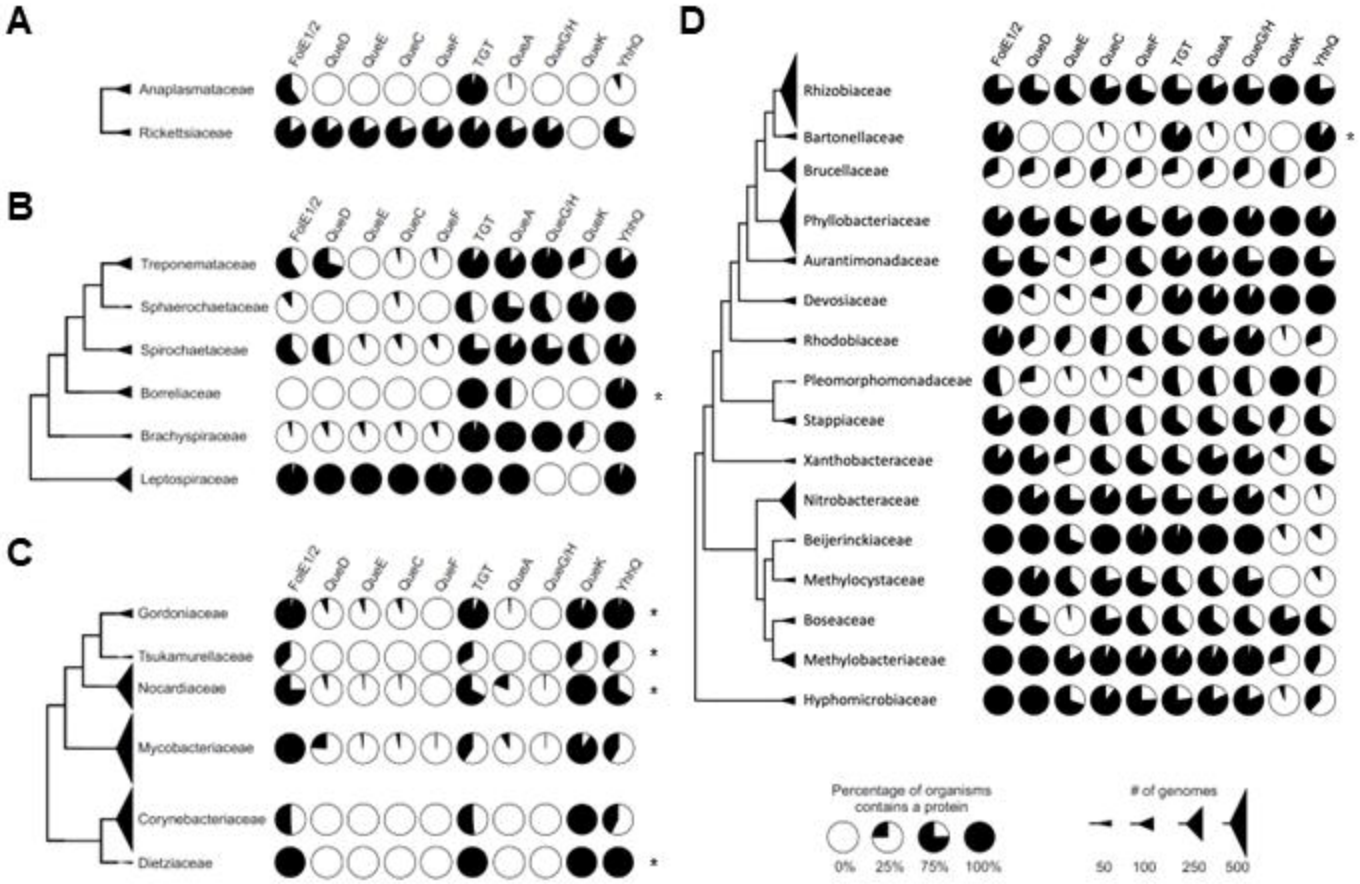
A
FolE1/2
QueD
QueE
QueC
QueF
TGT
QueA
QueG/H
QueK
YhhQ
Anaplasmataceae
Rickettsiaceae
B
Treponemataceae
Sphaerochaetaceae
Spirochaetaceae
Borreliaceae
Brachyspiraceae
Leptospiraceae
C
Gordoniaceae
Tsukamurellaceae
Nocardiaceae
Mycobacteriaceae
Corynebacteriaceae
Dietziaceae
D
Rhizobiaceae
Bartonellaceae
Brucellaceae
Phyllobacteriaceae
Aurantimonadaceae
Devosiaceae
Rhodobiaceae
Pleomorphomonadaceae
Stappiaceae
Xanthobacteraceae
Nitrobacteraceae
Beijerinckiaceae
Methylocystaceae
Boseaceae
Methylobacteriaceae
Hyphomicrobiaceae
Percentage of organisms contains a protein
0%
25%
75%
100%
# of genomes
50
100
250
500